Determination of volumetric cerebrospinal fluid absorption into extracranial lymphatics in sheep

M. BOULTON, M. FLESSNER, D. ARMSTRONG, J. HAY, AND M. JOHNSTON
Trauma Research Program and Department of Pathology, Sunnybrook Health Science Centre, University of Toronto, Toronto, Ontario, Canada M4N 3M5; and Department of Medicine, University of Rochester, Rochester, New York 14642

Boulton, M., M. Flessner, D. Armstrong, J. Hay, and M. Johnston. Determination of volumetric cerebrospinal fluid absorption into extracranial lymphatics in sheep. *Am. J. Physiol.* 274 (*Regulatory Integrative Comp. Physiol.* 43): R88–R96, 1998.—We estimated the volumetric clearance of cerebrospinal fluid (CSF) through arachnoid villi and extracranial lymphatics in conscious sheep. Catheters were inserted into both lateral ventricles, the cisterna magna, multiple cervical lymphatics, thoracic duct, and jugular vein. Uncannulated cervical vessels were ligated. ^{125}I-labeled human serum albumin (HSA) was administered into both lateral ventricles. ^{131}I-HSA was injected intravenously to permit calculation of plasma tracer loss and tracer recirculation into lymphatics. From mass balance equations, total volumetric absorption of CSF averaged 3.37 ± 0.38 ml/h, with 2.03 ± 0.29 ml/h (~60%) removed by arachnoid villi and 1.35 ± 0.46 ml/h (~40%) cleared by lymphatics. With projected estimates for noncannulated ducts, total CSF absorption increased to 3.89 ± 0.33 ml/h, with 1.86 ± 0.49 ml/h (48%) absorbed by lymphatics. Additionally, we calculated total CSF drainage to be 3.48 ± 0.52 ml/h, with 54 and 46% removed by arachnoid villi and lymphatics, respectively, using previously published mass transport data from our group. We employed estimates of CSF tracer concentrations that were extrapolated from relationships observed in the study reported here. We conclude that 40–48% of the total volume of CSF absorbed from the cranial compartment is removed by extracranial lymphatic vessels.

cerebrospinal fluid drainage; arachnoid villi; brain; spinal cord; lymph nodes; lymphatic vessels

THE CENTRAL NERVOUS SYSTEM (CNS) does not contain lymphatic vessels, and, as a consequence, it has been assumed that the lymphatic circulatory system does not play any role in the drainage of extracellular fluid from the CNS. Drainage of cerebrospinal fluid (CSF) into the venous system is thought to occur largely through the arachnoid villi (reviewed in Ref. 10). However, it has been known for some time that tracers injected into CSF or CNS parenchyma enter several lymphatics, especially those vessels in the head and neck region (reviewed in Ref. 5).

In a previous report from our group, radiolabeled albumin was administered into the lateral ventricles or into the lumbar CSF of conscious sheep. The lymphatics that drained the brain and spinal cord were mapped by monitoring the presence of the CSF tracer in various lymph nodes and by collecting lymph from a variety of cannulated vessels (3). Many lymphatic routes were identified, but the primary pathways were associated with the retropharyngeal-cervical nodes draining the brain and the intercostal and lumbar nodes draining the spinal cord. If lymphatics play an important role in the drainage of CSF, a significant drop in the plasma appearance of an intraventricularly injected tracer should be observed in the same animal after vessel ligation or diversion of lymph from the relevant lymphatic ducts. This was observed in a subsequent investigation. With lymph channels intact, we observed a mass transport rate into plasma normalized to the injected dose of 6.4 ± 1.0%/h leading to an average 6-h plasma recovery of 38.2 ± 5.7%. After diversion/ligation of the relevant lymphatic vessels, the values dropped to 2.9 ± 0.5%/h and 17.7 ± 2.7%, respectively (2). These results demonstrated that extracranial lymphatic vessels in sheep transported approximately one-half of the protein tracer from the CSF compartment into plasma.

The tracer recovery data in cats (4), rabbits (6, 7, 19), and sheep (2, 3) suggest an important role for lymphatics in the clearance of CSF protein. However, the possibility that lymphatics remove a significant volume of CSF has never been assessed. The objective of the studies outlined in this report was to use tracer recovery data to make estimates of CSF volumetric clearance through arachnoid villi and extracranial lymphatics. To achieve this, mass balances were carried out around the plasma, the retropharyngeal-cervical lymph pathway, and the thoracic duct and the resulting series of differential equations were solved simultaneously to provide a method to calculate the rates of fluid transfer from experimental data. The concentration of an intraventricularly injected protein tracer was measured in the CSF, plasma, and lymph compartments versus time, and the lymphatic flow rates were recorded. These data were inserted into the derived equations to provide estimates of the CSF flow rates through the arachnoid villi and via lymphatic drainage pathways.

MATERIALS AND METHODS

Surgery

Randomly bred female sheep (25–30 kg) were used in this investigation. Experiments were approved by the ethics committee at the Sunnybrook Health Science Center and conformed to the guidelines set by the Canadian Council on Animal Care and the Animals for Research Act of Ontario. Access to the CSF, blood, and lymph compartments was achieved as described by Boulton et al. (2). Briefly, under fluothane anesthesia, catheters were inserted into both lateral ventricles. Two ⅛-in. burr holes were made bilaterally, 1.5 cm anterior and 1.5 cm lateral to the posterior fontanelle. A single catheter guide screw was inserted into each hole. A 16-gauge Novalon intravenous catheter (Becton Dickinson, Sandy, UT) was then attached to a column of artificial CSF and fed through the guide screw. Entry of the catheter into

0363-6119/98 $5.00

the lateral ventricle was confirmed by a sudden drop in artificial CSF volume in the column. For access to the cisterna magna, a laminectomy of C1 was performed. A polyethylene catheter (ID 1.0 mm, OD 1.5 mm) was inserted through the meninges and fed cephalad along the subarachnoid space into the cisterna magna. The catheter was secured to the dura and exteriorized. The animals were allowed to recover for 3 days before experiments were performed.

On the day of the experiment, the thoracic duct, at its junction with the venous system, multiple cervical lymphatics, and left jugular vein were cannulated (thoracic duct catheter, ID 1.0 mm, OD 1.5 mm; cervical catheters, ID 0.58 mm, OD 0.96 mm; Critchley, Silverwater, Australia). In most animals, distinct right and left cervical ducts were visible, and in some sheep, multiple cervical ducts could be identified. Any cervical vessels that were too small to cannulate were ligated to prevent transport of the CSF tracer to plasma. The lymph from multiple cervical catheters was collected into a single bottle to pool the results from these vessels. Bottle holders were sutured to the animal, and lymph was collected in sterile plastic bottles with heparin added (~15 U/ml) to prevent coagulation. The outflow ends of all lymphatic catheters were positioned to be approximately level with the sheep's olecranon (near the level of the left atrium).

The sheep were allowed to recover from the anesthetic for 3–4 h and were fully conscious and standing in the cages. During experiments, lymph was collected hourly for 6 h. A 1.0-ml blood sample from the left jugular vein was also obtained at hourly intervals. Radioactivity was determined using a multichannel gamma spectrometer (Compugamma, LKB Wallac, Turku, Finland) with appropriate window settings and background subtraction.

Tracers and Solutions

^{125}I-labeled human serum albumin (^{125}I-HSA, 0.93 MBq/ml, 10 mg/ml) and ^{131}I-labeled HSA (37 MBq/ml, 10 mg/ml) were obtained from Frosst (Kirkland, Quebec, Canada). All tracer solutions were purified before use by passage through a Centricon centrifugal concentrator (10,000 mol wt cut off) to remove free ^{125}I or ^{131}I before infusion. To ensure that the measured radioactivity in any collected sample was protein associated, a second set of aliquots was assayed after precipitation with 10% trichloroacetic acid. Free or nonprotein-associated ^{125}I or ^{131}I represented <1% of the total radioactivity in any sample. Lactated Ringer solution was purchased from Baxter (Chicago, IL). Artificial CSF was made as described by Chodobski et al. (8).

Mathematical Model

Figure 1 outlines the essential features of a conceptual model that integrates brain lymph and arachnoid villi drainage systems with the CSF and vascular compartments. All compartments are assumed to be well mixed with no spatial variation of tracer concentration after injection or intercompartmental transfer. It is assumed that there is no direct transport of tracer into CNS capillaries and that all tracer is removed from the CNS by arachnoid villi or extracranial lymphatics. All tracer concentrations (C) are dependent on time; however, compartmental volumes are assumed to remain constant. It is assumed that there is no sequestration or destruction of tracer protein in the retropharyngeal-cervical or thoracic duct lymph. Intercompartmental flow rates (L, F, and D) are assumed to remain constant during an experiment because the injection of tracer in a small volume would not be expected to perturb intracranial pressure.

At the initiation of the experiment, a flow marker (^{125}I-HSA) was infused into both lateral ventricles. This raises the

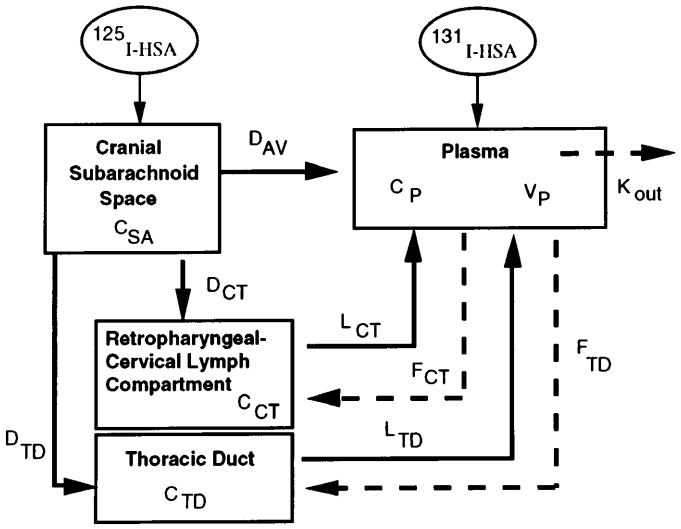

Fig. 1. Schematic illustrating essential features of a conceptual model that integrates arachnoid villi and lymphatic drainage systems with the cerebrospinal fluid (CSF) and vascular compartments. D_{AV}, rate of transport of CSF through the arachnoid villi (ml/h); D_{CT}, rate of transport of CSF into the retropharyngeal-cervical lymphatics (ml/h); D_{TD}, rate of transport of CSF into the thoracic duct (ml/h); C_{SA}, concentration of ^{125}I-labeled human serum albumin (HSA) in CSF [counts·min^{-1} (cpm)·ml^{-1}]; C_{CT}, concentration of ^{125}I- or ^{131}I-HSA in retropharyngeal-cervical lymph (cpm/ml); C_{TD}, concentration of ^{125}I- or ^{131}I-HSA in thoracic duct lymph (cpm/ml); C_P, concentration of ^{125}I- or ^{131}I-HSA in plasma (cpm/ml); L_{CT}, observed flow rate of retropharyngeal-cervical lymph (ml/h); L_{TD}, observed flow rate of thoracic duct lymph (ml/h); F_{CT}, volumetric transfer rate of the intraventricularly injected ^{131}I-HSA from the plasma into retropharyngeal-cervical lymph (ml/h); F_{TD}, volumetric transfer rate of the intraventricularly injected ^{131}I-HSA from the plasma into thoracic duct lymph (ml/h); V_P, volume of distribution of tracer in plasma.

subarachnoid concentration from $C_{SA}(0)$ to $C_{SA}(t)$. The flow marker transfers to the plasma via the arachnoid villi at a flow rate D_{AV}. Drainage also occurs to the retropharyngeal-cervical lymphatics at a flow rate of D_{CT} and to the thoracic duct at a rate of D_{TD}. The retropharyngeal-cervical lymphatics (tracer concentration = C_{CT}) receive fluid and solutes from the plasma at a rate of F_{CT}, whereas lymph flows to the plasma at rate L_{CT}. In the same fashion, the thoracic duct (tracer concentration = C_{TD}) receives fluid and solutes from the plasma at a flow rate of F_{TD}, whereas it drains to the plasma at a rate of L_{TD}. Flow marker concentrations within the plasma are designated C_P and distribute to the volume of distribution of the marker (V_P). The rate of transfer of a marker protein from the plasma to tissues other than those drained by the thoracic duct or retropharyngeal-cervical path occurs at a rate of $K_{out}(C_PV_P)$. A second label of the same flow marker injected into the CSF (^{131}I-HSA) is infused into the plasma space to estimate the flows from the plasma that are indicated with the dashed arrows in Fig. 1 (K_{out}, F_{CT}, F_{TD}). It is assumed that neither ^{125}I-HSA nor ^{131}I-HSA crosses the blood-brain barrier from the plasma into the CSF. The compartmental concentrations of the tracer have been designated by the superscripts 125 or 131 as appropriate.

Mass Balance Equations

A mass balance around the retropharyngeal-cervical lymph compartment assumes that the mass of tracer into the

compartment equals the mass flowing out. All concentrations are a function of time. The mass balance yields

$$D_{CT} = \frac{\int_0^t [L_{CT}C_{CT}^{125}(t) - F_{CT}C_P^{125}(t)]\,dt}{\int_0^t C_{SA}^{125}(t)\,dt}\ (ml/h) \qquad (1)$$

where C_{SA} is the concentration of tracer in CSF taken from the cisterna magna that reflects the mixed concentration of the CSF in the subarachnoid space; F_{CT} is the volumetric transfer rate of the intraventricularly injected tracer (^{125}I-HSA) from the plasma. It must be found from a balance around the cervical lymph compartment for the intravenously injected ^{131}I-HSA

$$F_{CT} = \frac{\int_0^t L_{CT}C_{CT}^{131}(t)\,dt}{\int_0^t C_P^{131}(t)\,dt}\ (ml/h) \qquad (2)$$

Mass balances around the thoracic duct for both tracers yield the following equations that can be used to calculate D_{TD} and F_{TD}

$$D_{TD} = \frac{\int_0^t [L_{TD}C_{TD}^{125}(t) - F_{TD}C_P^{125}(t)]\,dt}{\int_0^t C_{SA}^{125}(t)\,dt}\ (ml/h) \qquad (3)$$

and

$$F_{TD} = \frac{\int_0^t L_{TD}C_{TD}^{131}(t)\,dt}{\int_0^t C_P^{131}(t)\,dt}\ (ml/h) \qquad (4)$$

To obtain the value for arachnoid villi drainage (D_{AV}), a mass balance is performed around the blood

$$\frac{d(C_P^{125}V_P)}{dt} = D_{AV}C_{SA}^{125} + L_{CT}C_{CT}^{125} - K_{out}(C_P^{125}V_P) - F_{CT}C_P^{125} - F_{TD}C_P^{125} + L_{TD}C_{TD}^{125} \qquad (5)$$

where all concentrations are functions of time (t). On the assumption that V_P, F_{TD}, F_{CT}, and K_{out} are constant and that L_{TD} and L_{CT} are zero due to cannulation and collection of the lymph, the above equation takes the form

$$\frac{dC_P^{125}(t)}{dt} + \left(K_{out} + \frac{F_{CT} + F_{TD}}{V_P}\right)C_P^{125}(t) = \frac{D_{AV}C_{SA}^{125}(t)}{V_P} \qquad (6)$$

The observed plasma disappearance rate of ^{131}I-HSA is equal to $K_{exp}[V_P][C_P(t)]$ and

$$K_{exp} = \left(K_{out} + \frac{F_{CT} + F_{TD}}{V_P}\right) \qquad (7)$$

Substituting into *Eq. 6*

$$\frac{dC_P^{125}(t)}{dt} + K_{exp}C_P^{125}(t) = \frac{D_{AV}C_{SA}^{125}(t)}{V_P} \qquad (8)$$

This can be integrated between $t = 0$ and $t = t_f$

$$C_P^{125}(t_f)e^{K_{exp}t_f} - C_P^{125}(0) = \int_0^{t_f}\left[\frac{D_{AV}C_{SA}^{125}(t)}{V_P}\right]e^{K_{exp}t_f}\,dt \qquad (9)$$

Solving this equation for D_{AV}

$$D_{AV} = \left[\frac{C_P^{125}(t_f)e^{K_{exp}t_f} - C_P^{125}(0)}{\int_0^{t_f}\frac{C_{SA}^{125}(t)}{V_P}e^{K_{exp}t}\,dt}\right](ml/h) \qquad (10)$$

Experimental Design

A total of 10 mg of ^{125}I-HSA was injected in 2 × 500 μl portions into each lateral ventricle. At the same time, a second tracer (^{131}I-HSA) was injected into the venous circulation to permit *1*) calculation of the plasma volume, V_P; *2*) determination of a coefficient of elimination from the plasma, K_{exp}; and *3*) estimation of the filtration of plasma tracer into the relevant lymph compartments, F_{CT} and F_{TD}. Radioactivity was monitored in CSF, plasma, and lymph over 6 h. Samples of CSF from the cisterna magna (10 μl) were taken every hour. Plasma samples (1.0 ml) were collected every 4 min for 30 min, at 60 min, and then hourly. Lymph from cervical lymphatics and the thoracic duct was collected continuously. A Macrodex saline solution (6% Dextran 70, Pharmacia) was infused into the jugular catheter in volumes equivalent to those lost from the diverted thoracic duct. Because all known lymphatic drainage pathways were diverted or ligated, the plasma recovery of tracer was assumed to be related to arachnoid villi drainage.

Method of Solution of Equations

To solve the equations, the following must be determined in experiments as functions of time: C_{SA} (from cisterna magna), L_{CT} and C_{CT} from direct cannulation and collection of the retropharyngeal-cervical lymph and L_{TD} and C_{TD} from direct cannulation and collection of thoracic duct lymph. C_P was determined from plasma concentrations, and V_P was calculated from the dilution of ^{131}I-HSA injected into the venous circulation as described in an earlier publication (1). K_{exp} was estimated from the ^{131}I-HSA plasma disappearance curve. Graphical integration was carried out using the trapezoidal rule (15).

Estimation of Lymphatic CSF Clearance in Uncannulated Lymphatics

In most experiments, we underestimated the contribution of lymphatics to CSF clearance because not all cervical lymphatics could be cannulated. Some vessels were too small to cannulate. In other cases, coagulation of lymph in the plastic catheters caused flow to cease. However, we made estimates for the contribution of these vessels to CSF absorption. In each preparation we noted the number of cervical ducts and measured their diameter. Flow rate in a vessel is the product of velocity and cross-sectional area. If we assume that the velocity of the lymph in all cervical vessels was the same, then flow would be proportional to diameter (d) squared or d^2. To obtain an estimate for the CSF drainage into uncannulated cervical vessels (D_{CT}^u) using measured values from cannulated ducts ($D_{CT}^{measured}$), we used the following approach

$$D_{CT}^u = \left[\frac{D_{CT}^{measured}}{\text{no. cannulated vessels}}\right] \times \left[\frac{d_u}{d_c}\right]^2 \times \text{no. uncannulated vessels} \qquad (11)$$

where d_u and d_c represent the diameter of the uncannulated and cannulated vessels, respectively. In these estimations, we

assumed that the concentration of tracer was similar in all ducts.

Estimation of Arachnoid Villi and Lymphatic CSF Volumetric Clearance from Mass Transport Studies Previously Published by Our Group

We also used data published previously by our group (2) to make additional estimates of volumetric CSF clearance through arachnoid villi and lymphatic vessels. In the former study, we calculated a mass transport rate (%injected tracer/h from CSF to plasma) of an intraventricularly administered protein before and after lymph diversion/ligation in the same conscious sheep. Cisterna magna tracer concentrations (C_{SA}; which represent the mixed concentration of the tracer in subarachnoid CSF) were not monitored, and therefore, we could not originally calculate volumetric flow rates. However, C_{SA} can be estimated from the data reported here. From the data generated in this study, we expressed C_{SA} as a percentage of the injected amount per milliliter and plotted the mean values over time. A consistent level of tracer dilution and an exponential decline in concentration were observed. Because the total amount of tracer injected into each animal was known in the previously published mass transport report, we calculated C_{SA} for each time using the equation of the best fit line through the CSF tracer disappearance curve.

In *phase 2* of the experiments published previously, lymph was diverted or the vessels were ligated. With the use of estimates for C_{SA}, *Eq. 10* was used to calculate volumetric flow rates through arachnoid villi. In *phase 1* of the experiment, lymphatics were left intact. Therefore, calculations of flow rates with *Eq. 10* under these circumstances were used to determine the sum of transport via arachnoid villi and lymphatic vessels. The difference between *phase 1* and *2* values provided an estimate of the lymphatic contribution to CSF absorption.

All data were expressed as means ± SE. In Figs. 2–4, *t*(0) represents the time that the tracers were injected into the CSF and plasma compartments. The results were analyzed with analysis of variance. In some cases, the data were assessed with a paired Student's *t*-test. We interpreted $P < 0.05$ as significant.

RESULTS

Of the 10 sheep used for this study, 6 had sufficient information for data analysis. That is, at least one cervical lymphatic and the thoracic duct were flowing and blood and CSF samples were collected successfully. One animal was removed from analysis because of red blood cells in the CSF. The background physiological data for all animals are illustrated in Table 1.

Table 1. *Animal data*

Sheep No.	Plasma Volume, ml	K_{exp}	Mean Cervical Lymph Flow Rate, ml/h*	Mean Thoracic Duct Lymph Flow Rate, ml/h*
032	1,582	0.059	2.3	69
020	1,188	0.058	3.9	105
062	1,050	0.074	2.1	78
023	1,298	0.063	8.4	73
082	1,465	0.064	21.0	79
048	1,025	0.064	17.1	62
Mean ± SE	1,268 ± 92	0.064 ± 0.002	9.1 ± 3.3	78.0 ± 6.0

K_{exp}, coefficient of elimination from plasma. *Averaged over 6 h.

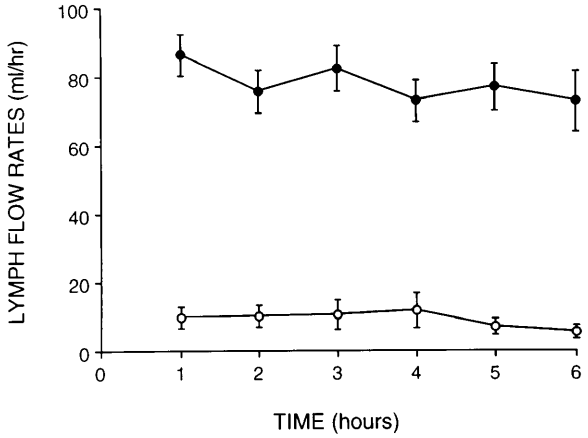

Fig. 2. Cervical (○) and thoracic duct (●) flow rates ($n = 6$). A 1-way repeated-measures analysis of variance with Greenhouse-Geisser adjusted *P* values revealed no significant changes in flow rates in either vessel over time.

The lymph flow rates monitored over 6 h in the cannulated lymphatics are illustrated in Fig. 2. These flows represent lymph transport from all tissues, not just fluid originating as CSF. There were no significant changes in thoracic duct or cervical lymphatic flow rates over the 6-h duration of the experiment.

After injection of ^{125}I-HSA into the lateral ventricles, radioactivity was detected in cisterna magna CSF, cervical and thoracic duct lymph, and blood. An example of the data from one sheep is illustrated in Fig. 3. In all but one animal, the concentration of ^{125}I-HSA in cisterna magna showed an exponential decline. In one sheep (*032*), the tracer concentration increased up to 3 h and declined after this point. The highest concentration of intraventricularly administered tracer outside the CNS was observed in cervical lymph in all but one animal (*032*). The plasma concentration of the ^{131}I-HSA injected intravenously declined exponentially, and this tracer was observed in cervical and thoracic duct lymph.

Estimates of Volumetric CSF Drainage Via Arachnoid Villi and Extracranial Lymphatic Vessels

Table 2 illustrates the calculated volume data from the mass balance equations. With the cervical and thoracic duct lymph diverted from the animal (or with some of the smaller cervical vessels ligated), the recovery of intraventricularly administered tracer in the plasma was attributed to transport via the arachnoid villi, and D_{AV} was calculated using *Eq. 10*. Arachnoid villi volume transport rates ranged from 0.70 to 2.67 ml/h. There was considerable variation in the volume transport rates calculated for the cannulated cervical lymphatics (D_{CT} ranged from 0.09 to 2.74 ml/h). In one animal, the CSF volume transport into the thoracic duct was relatively high ($D_{TD} = 2.49$ ml/h), but in the other sheep estimated flow rates were low (0.00 to 0.4 ml/h). Total CSF absorption (sum of D_{AV}, D_{CT}, and D_{TD}) averaged 3.37 ± 0.38 ml/h, with 2.03 ± 0.29 ml/h being removed by arachnoid villi and 1.35 ± 0.46 ml/h cleared by extracranial lymphatics.

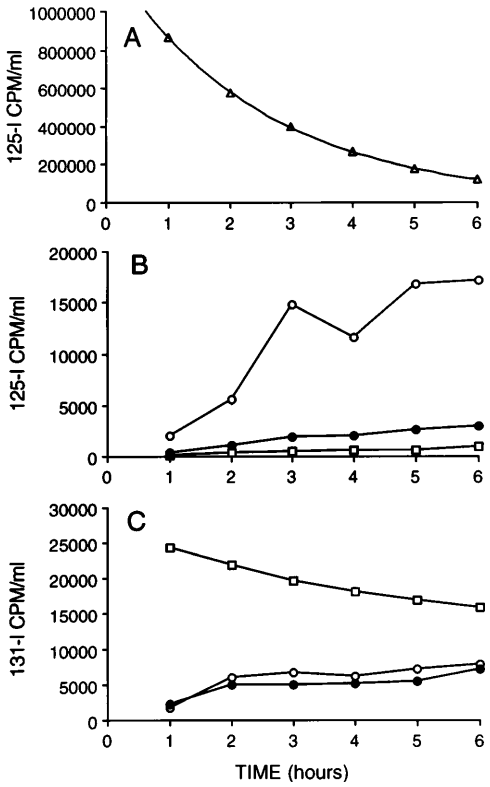

Fig. 3. Example of compartmental HSA concentrations in CSF, plasma, and lymph (*sheep 082*; Tables 1, 2, and 3). *A*: ^{125}I-HSA concentrations in cisterna magna CSF. *B*: ^{125}I-HSA concentrations in retropharyngeal-cervical lymph (○), thoracic duct (●), and plasma (□). *C*: ^{131}I-HSA concentrations in retropharyngeal-cervical lymph (○), thoracic duct (●), and plasma (□).

These experiments will have underestimated the contribution of lymphatics to CSF clearance because not all cervical lymphatics could be cannulated. Using methods described earlier, we estimated CSF absorption into uncannulated ducts (D^{u}_{CT} in Table 3). Total cervical CSF drainage was projected as the sum of D^{u}_{CT} and measured cervical values obtained from cannulated vessels in the same animal ($D^{measured}_{CT}$). Arachnoid villi absorption remained at 2.03 ± 0.29 ml/h. Total lymph clearance rates increased to 1.86 ± 0.49 ml/h, and as a consequence, estimates for the sum of clearance via all pathways also increased to 3.89 ± 0.33 ml/h.

Table 2. *Calculated volumetric data from cannulated animals*

Sheep No.	D_{AV}, ml/h	D_{CT}, ml/h	D_{TD}, ml/h	Total Lymph, ml/h	D_{AV} + Lymph
032	2.29	0.09	2.49	2.58	4.87
020	2.67	0.15	0.05	0.20	2.87
062	2.42	1.15	0.40	1.55	3.97
023	1.75	0.50	0.00	0.50	2.25
082	2.32	0.51	0.01	0.52	2.84
048	0.70	2.74	0.00	2.74	3.44
Mean	2.03	0.86	0.49	1.35	3.37
±SE	0.29	0.41	0.40	0.46	0.38

D_{AV}, rate of transport of cerebrospinal fluid (CSF) through the arachnoid villi; D_{CT}, rate of transport of CSF into retropharyngeal-cervical lymphatics; D_{TD}, rate of transport into thoracic duct.

Estimates of Volumetric CSF Drainage Into Lymphatics Using Previously Published Mass Transport Data

Figure 4 illustrates the mean cisterna magna tracer concentrations as a percentage of the injected amount plotted over time. The data from *sheep 032* were omitted. Knowing the total amount of tracer injected in the report published previously, we estimated C_{SA} from the C_{SA} versus time relationship observed in the present study. Before lymph diversion/ligation we estimated CSF absorption to be 3.48 ± 0.52 ml/h, and after diversion/ligation, values dropped significantly to 1.62 ± 0.25 ml/h (Table 4). The latter value is an estimate of arachnoid villi drainage. The difference between *phase 1* and *phase 2* (1.86 ± 0.48 ml/h) represents an estimate of the contribution of extracranial lymphatics. In sham-operated animals, no significant differences between volume flows were observed, although the estimated volume transport values were ~14% less in *phase 2* of the experiments.

DISCUSSION

In this report, we used tracer recovery data to estimate the volumetric clearance of CSF through arachnoid villi and extracranial lymphatics. An important element in the design of the mathematical model was the ability to correct the recovery data for errors introduced by filtration. This correction was significant because, on average, the loss of tracer from sheep plasma was over 6%/h. Because plasma recoveries in lymph-diverted animals were used to estimate arachnoid villi drainage, tracer loss would result in this pathway being underestimated. Similarly, the transport of tracer to the plasma complicates measurements of the CSF tracer in lymph because the HSA that was transported from the CSF into plasma by the arachnoid villi would filter back into the lymphatic compartment, resulting in an overestimate of the lymphatic contribution to CSF drainage. With these filtration factors accounted for, the data suggested that 40–48% of all CSF removed from the cranial compartment in sheep was cleared by lymphatics. Therefore, extracranial lymphatic vessels have a major role in CSF volumetric clearance in this species. However, some comment should be made about the conceptual basis for the mathematical model and the assumptions necessary for the derivation of the equations.

Methodological Considerations

Conceptual model. The mass balance equations used in this study were based on a relatively simple three-compartment model (CSF, plasma, and extracranial lymph). It was assumed that fluid transfer occurred directly from one compartment to another. However, the model can be refined further depending on the outcome of continuing studies that address several experimental and anatomical issues. For example, if the majority of tracer in cervical lymph came from the CSF compartment, then the cervical lymph tracer concentration should parallel the CSF concentration.

Table 3. *Projected estimates of CSF drainage into noncannulated cervical lymphatics*

Sheep No.	No. Cervicals Cannulated/ No. Identified (size cannulated vessel, mm)	$D_{CT}^{measured}$,* ml/h	Uncannulated Ducts, No. (size mm)	D_{CT}^{u}	Projected D_{CT}† Total	Projected D_{CT}† + D_{TD},* ml/h	Projected D_{CT}† + D_{AV}* + D_{TD},* ml/h
032	2/2 (1.0)	0.09	none	0.0	0.09	2.58	4.87
020	2/6 (1.0)	0.15	4 (0.5)	0.08	0.23	0.28	2.95
062	2/3 (1.0)	1.15	1 (1.0)	0.58	1.73	2.13	4.55
023	1/3 (1.0)	0.50	2 (1.0)	1.0	1.50	1.50	3.25
082	2/4 (1.0)	0.51	2 (1.0)	0.51	1.02	1.03	3.35
048	3/4 (1.0)	2.74	1 (1.0)	0.91	3.65	3.65	4.35
Mean ± SE		0.86 ± 0.41		0.51 ± 0.17	1.37 ± 0.53	1.86 ± 0.49	3.89 ± 0.33

Estimate for CSF drainage into uncannulated cervical vessels (D_{CT}^{u}) using measured values from cannulated ducts ($D_{CT}^{measured}$). *Taken from Table 2; †$D_{CT}^{u} + D_{CT}^{measured}$.

This was not the pattern that was observed. The time course of the tracer concentration in cervical lymph was different from that in the CSF as can be seen in the example illustrated in Fig. 3.

The observation that cervical tracer concentration increased, whereas the tracer concentration in CSF declined could be explained by a delay in the equilibration of the tracer in CSF. In our studies, radioactive albumin was injected into both lateral ventricles. The ideal situation would have this tracer equilibrate instantaneously in the CSF compartment. However, it may take some time for the protein to equilibrate in the CSF close to the nasal submucosa. This could account for the observed tracer patterns.

Alternatively, CSF may not transport directly to cervical lymph but rather may mix in the fluid volume of an intermediate compartment. Unfortunately, the exact anatomic relationships between CSF and cervical lymph in sheep are unknown. In rats, an intermediate compartment does not appear to exist, as CSF tracers pass through arachnoid channels directly into nasal lymphatics (12). In other species, tracers injected into the CSF transport along the prolongations of the subarachnoid space around certain cranial and spinal nerves. These perineural extensions of the subarachnoid space open into the tissue spaces from which the tracer is absorbed into prenodal lymphatics (9). In the case of the cervical lymphatic vessels, the potential intermediate compartment would be the nasal submucosa. Because our estimates of lymphatic CSF clearance depend on the amount of tracer collected in cervical lymph, any delay in the passage of the tracer from the CSF to the cannulated vessel (as tracer equilibrates in a potential intermediate compartment) may result in underestimated values for lymphatic absorption. As details of the anatomic connections between CSF and cervical lymph are revealed, the development of a more complex four-compartment model may facilitate our understanding of CSF transport into extracranial lymphatic vessels.

Mathematical assumptions. In deriving the mass balance equations, we have assumed that the volumetric flow rates defined by the letters L, D, and F remained constant for the duration of the experiment. The observed thoracic duct and cervical lymphatic flow rates were relatively stable over the 6-h duration of the experiments (Fig. 2). Injection volumes and sample collections were small to prevent effects on CSF pressures, which could alter the volume transfer of CSF (D).

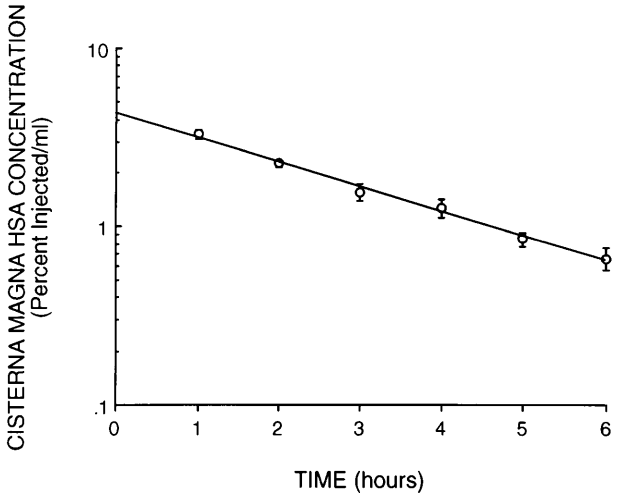

Fig. 4. Tracer concentrations in the cisterna magna ($n = 5$).

Table 4. *Volumetric estimates from mass transport data*

Sheep No.	Estimated Volume Transport, ml/h *Phase 1*	*Phase 2*
	Lymph-diverted sheep	
1	1.73	0.79
2	2.89	0.93
3	3.07	1.58
4	5.20	2.40
5	2.63	1.91
6	5.52	1.30
7	3.33	2.46
Mean ± SE	3.48 ± 0.52	1.62 ± 0.25*
	Sham-operated sheep	
8	1.52	2.26
9	3.84	3.41
10	4.01	2.93
11	2.27	1.94
12	5.90	4.65
13	6.83	5.73
Mean ± SE	4.06 ± 0.83	3.49 ± 0.59

*$P < 0.05$.

The slope of the plasma disappearance curve of intravenously injected ^{131}I-HSA was used to calculate a coefficient of elimination for labeled HSA and to permit correction for the plasma tracer (and accompanying volume) that refiltered into the lymphatics. The disappearance of tracer followed a typical exponential decline. The amount of tracer (and volume) entering the lymphatic compartment from the plasma would be defined by the filtration coefficient for each tissue compartment. No physiological perturbations were attempted in these experiments, and, therefore, the volumetric transfer of ^{131}I-HSA (F) would not be expected to change.

Properties of the CSF tracer. We assumed that albumin moves from the CSF into the arachnoid villi or lymphatics with little or no tracer exiting the CNS by other routes. Other potential exit pathways for the tracer include blood capillaries in the brain, the choroid plexus, and diffuse drainage along the arachnoid membrane (reviewed in Ref. 14). Because very little transport of protein occurs across blood capillaries into the brain (5), it also seems reasonable to assume that little direct albumin transfer from the CSF into blood occurs. Experimental data support this assumption (13, 16). The choroid plexus is thought to be responsible for some drainage, although the magnitude of this clearance is unknown (18). It seems unlikely that HSA is removed from the CSF through this route, but, if this were the case, our model would interpret this as transport of tracer by the arachnoid villi. Larger molecules do not appear to escape directly through the arachnoid membrane under physiological pressures (14). At high pressures, large tracers may penetrate the arachnoid membrane and enter the extracellular space of the dura mater. We did not elevate intracranial pressures in these experiments, and, therefore, we suspect that little CSF tracer escaped via this route. However, if any of the tracer passed through the arachnoid membrane it would likely be taken up by dural lymphatic vessels.

Relevance of anatomic variations to estimates of CSF volumetric clearance via lymphatics. A limitation of the model used in this report relates to the variability of the lymphatic drainage pathways and the lack of access to some of the smaller cervical vessels. In the cases in which we identified the relevant cervical ducts and ligated the smaller vessels, the lymph contribution to CSF clearance would be underestimated by an unknown amount. In Table 3, we estimated the contribution of the ligated vessels. We had to assume that the tracer concentration in the ligated cervical ducts was similar to that in the cannulated vessels. Equal amounts of the HSA were injected into both lateral ventricles, thereby increasing the possibility that the tracer would be distributed equally to all extracranial tissue compartments drained by the retropharyngeal-cervical lymphatics. However, this could not be confirmed experimentally.

In regard to the issue of anatomic variation, *sheep 032* was an interesting animal because the thoracic duct contained much more CSF tracer than the cervical vessels. Normally, it would appear that the cervical ducts empty into the veins at the base of the neck separate from the thoracic duct. However, in this animal the cervicals appeared to empty into the thoracic duct upstream of our cannulation point. Therefore, this sheep may provide a more realistic estimate of the total cervical contribution to CSF drainage (~50%).

Another problem relates to cervical lymphatics that may not have been identified during the surgical procedures. If present, these nonligated vessels would transport CSF tracer to the plasma and inflate the arachnoid villi value. Similarly, the right lymph duct, which we did not cannulate, may contribute to CSF clearance. In sheep, this duct does not appear to be present in every animal. In the experiments reported here, we attempted to identify, cannulate, or ligate this vessel. In only one experiment were we able to collect lymph for any period of time, and no significant CSF tracer was observed. Nonetheless, the right lymph duct has the potential to drain CSF, especially as the head and neck region represent its natural drainage basin. In summary, the volumetric estimates presented in this report have to be viewed in the context that the anatomic/surgical limitations of the model tend to underestimate the lymphatic and overestimate the arachnoid villi contribution to CSF clearance.

Magnitude of total CSF clearance. Total volumetric CSF absorption from the cranial cavity was estimated using two different approaches. If we consider the data based on the recovery of tracer in the plasma and in the collected lymph, we estimated a total mean CSF clearance of 3.37 ± 0.38 ml/h (range from 2.25 to 4.87 ml/h). This is clearly an underestimate because the contribution of the ligated lymphatic vessels was not taken into consideration. If we project estimates for the uncannulated lymphatics, these values increase to a mean of 3.89 ± 0.33 ml/h (range from 2.95 to 4.87 ml/h). Using the previously published mass transport data to estimate volumetric drainage we calculated a mean of 3.75 ± 0.46 ml/h (range from 1.52 to 6.83 ml/h). These latter values represent the 13 animals in *phase 1* of the experiments before lymph diversion/ligation or sham surgery. Taken together, it would appear that a realistic estimate for total CSF absorption would be just under 4 ml/h.

Because CSF formation and absorption would be expected to be equal in a steady state, we can compare our CSF clearance estimates with published values of CSF formation in sheep that were calculated using ventriculocisternal perfusion methods. In this technique, a known volume of artificial CSF containing a known concentration of tracer is infused into the lateral ventricles and the measurement of outflow volume and CSF tracer concentration is made from a cisternal or lumbar port. With blue dextran as the CSF marker, values of 118.4 ± 12.8 (11), 111.08 ± 17.6 (17), and 82.3 ± 1.7 μl/min (8) have been reported for the CSF formation rate (~4.9–7.1 ml/h).

Our estimates for CSF absorption are slightly below the average values for CSF formation rates reported in the literature. There are several factors that could account for this. Differences may exist in the CSF

dynamics between various breeds of sheep. In addition, we used sheep between 25 and 30 kg. In the only case in which details were given in the references noted above, the weights of the sheep ranged from 35 to 40 kg (8). One might expect that the larger, older animals would have greater CSF volumes and rates of secretion and absorption. Another explanation relates to the possibility that we underestimated the lymphatic component (and therefore the sum of arachnoid villi and lymphatic absorption) due to problems associated with the identification of all cervical vessels or assessment of the right lymph duct contribution. Nonetheless, we conclude that our method provides values for total CSF absorption/formation that are consistent with data in the literature derived with different techniques.

Proportion of CSF removed by arachnoid villi and extracranial lymphatic vessels. The proportion of CSF removed by extracranial lymphatics and arachnoid villi was quite variable. In two of the animals, CSF removal by lymphatics was greater than that estimated for arachnoid villi. In one case (*sheep 048*), ~80% of total CSF absorption was attributed to extracranial lymphatics. In the remaining animals, more CSF was cleared by arachnoid villi (in *sheep 020* for example, ~93% of CSF was absorbed by this route). If we ignore contributions of the uncannulated, ligated vessels, the most conservative estimates for the proportion of lymphatic clearance of CSF ranged from 7 to 80% (mean of ~40%; Table 5). If we estimate the contributions of the ligated vessels, the proportion of total CSF cleared by lymphatics ranged from 9 to 84% (mean 52% drainage through arachnoid villi and 48% through lymphatics).

From Table 2, it appears as though the lowest estimates for the lymphatic contribution came from animals in which the fewest cervical ducts were cannulated relative to the total number identified. In the three sheep in which one-half or fewer of the cervicals were cannulated, estimated flow rates were 0.5 ml/h or less. In the three animals with the majority of cervical ducts cannulated, the calculated flow rates were all >1.5 ml/h. Therefore, while biological variability no doubt contributed to the wide range of estimated CSF lymphatic clearances, an important consideration relates to difficulties in collecting lymph from multiple, small cervical vessels. If we had been able to collect lymph consistently from all cervical lymphatics, it is likely that less variation would have been observed. In any event, the data suggest collectively that extracranial lymphatics are responsible for 40–48% of total volumetric CSF clearance. In support of this, the calculated proportions from the two phase mass balance experiments were on average very similar (54% arachnoid villi, 46% lymphatic). For these latter estimates, we reduced the lymphatic component by 14% to reflect the small mean reduction in the mass transport rates observed in sham-operated animals (Table 4; this report and Ref. 2). The proportion of drainage through arachnoid villi and lymphatics estimated with three different methods is summarized in Table 5.

Table 5. *Proportion of total CSF clearance through arachnoid villi and lymphatics*

	Total CSF Clearance, ml/h	Arachnoid Villi, %	Extracranial Lymphatics, %
Cannulation experiments (lymph underestimate due to ligated vessels)	3.37	60	40
Projected values from cannulation experiments (estimates of contributions from ligated vessels added)	3.89	52	48
Calculated values from mass transport experiments (estimates for CSF tracer concentrations)	3.48*	54*†	46*†

*Mean of 7 animals from lymph diversion studies illustrated in Table 4. Values derived from data published previously (2). †In sham-operated animals, plasma recoveries dropped 14% although no lymphatic vessels were ligated or lymph diverted. Because the difference in plasma recoveries before and after lymph diversion/ligation was used to estimate volumetric clearance into lymphatics, lymph flow rates were reduced 14% to reflect the slight inhibition of mass transport that should not be attributed to extracranial lymphatic drainage.

The retropharyngeal-cervical ducts were clearly the most important lymphatics in cranial CSF drainage. Cervical flow rates averaged 9.1 ml/h (i.e., CSF-derived fluid plus fluid from other tissues). Our calculated CSF volumetric flows into these vessels averaged between 0.86 and 1.37 ml/h (Tables 2 and 3). This suggested that fluid originating as CSF represented between 9.5 and 15% of normal volume flow rates in these vessels. The thoracic duct was of minor importance in the clearance of cranial CSF but may assume greater importance in the drainage of spinal cord CSF, as was established in an earlier report from our group (3).

In summary, the concentration of an intraventricularly injected HSA in the CSF, plasma, and lymph compartments was used in conjunction with mass balance equations to estimate and compare the volumetric CSF clearance through arachnoid villi and extracranial lymphatics in adult sheep. We demonstrated that, on average, 40–48% of all CSF drained was removed by extracranial lymphatic vessels.

Perspectives

Despite the fact that a physiological relationship between CNS extracellular fluid, CSF, and extracranial lymph has been known for many years, it has been assumed that lymphatic vessels have little role in volumetric CSF clearance. This view is no longer tenable. The data in this report for the first time demonstrate that extracranial lymphatics in sheep remove nearly one-half of all CSF absorbed and, as a consequence, must be considered to participate in normal CNS fluid balance regulation. What is more remarkable is that, if anything, the lymphatic contribution may be underestimated. Given that it is very difficult to cannulate and even identify all retropharyngeal-cervical lymphatic vessels and that the role of the right lymph duct is unknown, it is possible that CSF absorption into lymphatics may be considerably greater. The results from this study have important implica-

tions. First, several pathophysiological states are characterized by elevated CSF outflow resistance, leading to increased intracranial pressure. In some cases, it has been assumed that the fault may lie at the level of arachnoid villi but consideration must now be given to the possibility that impaired lymphatic clearance may perturb normal intracranial pressure-volume relationships. Second, as other investigators have proposed, extracranial lymphatics may provide a link between the brain and the immune system (9). Many lymph nodes are located along lymphatic CSF drainage pathways (3), and these direct connections between the CNS and lymphoid tissue could have important neuroimmunological implications.

The authors thank Dr. J. P. Szalai (Department of Biostatistics, Sunnybrook Health Science Centre) for help in the statistical analysis of the data.

This research was funded by the Medical Research Council of Canada.

Address for reprint requests: M. G. Johnston, Trauma Research Program and Dept. of Pathology, Univ. of Toronto, Research Bldg., S-111, Sunnybrook Health Science Centre, 2075 Bayview Ave., Toronto, Ontario M4N 3M5.

Received 16 May 1997; accepted in final form 23 September 1997.

REFERENCES

1. **Abernethy, N. J., W. Chin, J. B. Hay, H. Rodela, D. Oreopoulos, and M. G. Johnston.** Lymphatic drainage of the peritoneal cavity in sheep. *Am. J. Physiol.* 260 (*Renal Fluid Electrolyte Physiol.* 29): F353–F358, 1991.
2. **Boulton, M., M. F. Flessner, D. Armstrong, J. B. Hay, and M. G. Johnston.** Lymphatic drainage of the CNS: effects of lymph diversion/ligation on CSF protein transport to plasma. *Am. J. Physiol.* 272 (*Regulatory Integrative Comp. Physiol.* 41): R1613–R1619, 1997.
3. **Boulton, M., A. Young, J. B. Hay, D. Armstrong, M. Flessner, M. Schwartz, and M. G. Johnston.** Drainage of CSF through lymphatic pathways and arachnoid villi in sheep: measurement of ^{125}I-albumin clearance. *Neuropathol. Appl. Neurobiol.* 22: 325–333, 1996.
4. **Bradbury, M. W. B., and D. F. Cole.** The role of the lymphatic system in drainage of cerebrospinal fluid and aqueous humour. *J. Physiol. (Lond.)* 299: 353–365, 1980.
5. **Bradbury, M. W. B., and H. F. Cserr.** Drainage of cerebral interstitial fluid and of cerebrospinal fluid into lymphatics. In: *Experimental Biology of the Lymphatic Circulation 9*, edited by M. G. Johnston. Amsterdam: Elsevier, 1985, p. 355–394.
6. **Bradbury, M. W. B., H. F. Cserr, and R. J. Westrop.** Drainage of cerebral interstitial fluid into deep cervical lymph of the rabbit. *Am. J. Physiol.* 240 (*Renal Fluid Electrolyte Physiol.* 9): F329–F336, 1981.
7. **Bradbury, M. W. B., and R. J. Westrop.** Factors influencing exit of substances from cerebrospinal fluid into deep cervical lymph of the rabbit. *J. Physiol. (Lond.)* 339: 519–534, 1983.
8. **Chodobski, A., J. Szmydynger-Chodobska, E. Cooper, and M. J. McKinley.** Atrial natriuretic peptide does not alter cerebrospinal fluid formation in sheep. *Am. J. Physiol.* 262 (*Regulatory Integrative Comp. Physiol.* 31): R860–R864, 1992.
9. **Cserr, H. F., and P. M. Knopf.** Cervical lymphatics, the blood-brain barrier and the immunoreactivity of the brain: a new view. *Immunol. Today* 13: 507–512, 1992.
10. **Davson, H., K. Welch, and M. B. Segal.** *Physiology and Pathophysiology of the Cerebrospinal Fluid*. New York: Churchill Livingstone, 1987.
11. **Evans, C. A. N., J. M. Reynolds, M. L. Reynolds, N. R. Saunders, and M. B. Segal.** The development of a blood-brain barrier mechanism in foetal sheep. *J. Physiol. (Lond.)* 238: 371–386, 1974.
12. **Kida, S., A. Pantazis, and R. O. Weller.** CSF drains directly from the subarachnoid space into nasal lymphatics in the rat. Anatomy, histology and immunological significance. *Neuropathol. Appl. Neurobiol.* 19: 480–488, 1993.
13. **Marmarou, A., G. Hochwald, T. Nakamura, K. Tanaka, J. Weaver, and J. Dunbar.** Brain edema resolution by CSF pathways and brain vasculature in cats. *Am. J. Physiol.* 267 (*Heart Circ. Physiol.* 36): H514–H520, 1994.
14. **McComb, J. G.** Recent research into the nature of cerebrospinal fluid formation and absorption. *J. Neurosurg.* 59: 369–383, 1983.
15. **McCracken, D. D., and W. S. Dorn.** *Numerical Methods and Fortran Programming.* New York: Wiley, 1964, p. 162.
16. **Ohata, K., A. Marmarou, and J. T. Povlishock.** An immunocytochemical study of protein clearance in brain infusion edema. *Acta Neuropathol. (Berl.)* 81: 162–177, 1990.
17. **Payne, R., J. Madsen, R. C. Harvey, and C. E. Inturrisi.** A chronic sheep preparation for the study of drug pharmacokinetics in spinal and ventricular CSF. *J. Pharmacol. Methods* 16: 277–296, 1986.
18. **Van Deurs, B.** Structural aspects of brain barriers with special reference to the permeability of the cerebral endothelium and choroidal epithelium. *Int. Rev. Cytol.* 65: 117–191, 1980.
19. **Yamada, S., M. DePasquale, C. S. Patlak, and H. F. Cserr.** Albumin outflow into deep cervical lymph from different regions of rabbit brain. *Am. J. Physiol.* 261 (*Heart Circ. Physiol.* 30): H1197–H1204, 1991.